Accelerating oscillatory fronts in a nonlinear sonic vacuum with strong nonlocal effects

O. V. Gendelman,[1,*] V. Zolotarevskiy,[1] A. V. Savin,[2] L. A. Bergman,[3] and A. F. Vakakis[4]

[1]*Faculty of Mechanical Engineering, Technion–Israel Institute of Technology, Haifa 32000, Israel*

[2]*Semenov Institute of Chemical Physics, Russian Academy of Sciences, Moscow 119991, Russia*

[3]*Department of Aerospace Engineering, University of Illinois in Urbana-Champaign, USA*

[4]*Department of Mechanical Science and Engineering, University of Illinois in Urbana-Champaign, USA*

(Received 10 June 2015; revised manuscript received 18 October 2015; published 15 March 2016)

We describe and explore accelerating oscillatory fronts in sonic vacua with nonlocal interactions. As an example, a chain of particles oscillating in the plane and coupled by linear springs, with fixed ends, is considered. When one end of this system is harmonically excited in the transverse direction, one observes accelerated propagation of the excitation front, accompanied by an almost monochromatic oscillatory tail. Position of the front obeys the scaling law $l(t) \sim t^{4/3}$. The frequency of the oscillatory tail remains constant, and the wavelength scales as $\lambda \sim t^{1/3}$. These scaling laws result from the nonlocal effects; we derive them analytically (including the scaling coefficients) from a continuum approximation. Moreover, a certain threshold excitation amplitude is required in order to initiate the front propagation. The initiation threshold is evaluated on the basis of a simplified discrete model, further reduced to a completely integrable nonlinear system. Given their simplicity, nonlinear sonic vacua of the type considered herein should be common in periodic lattices.

DOI: 10.1103/PhysRevE.93.032216

I. INTRODUCTION AND DESCRIPTION OF THE MODEL

Nonlocal nonlinearities naturally appear in classical models describing the nonlinear motion of beams with restrained ends [1,2]. For example, the transverse dynamics of a beam with fixed ends, bending in a direction of one of the main axes of its cross section, is described by the following partial integrodifferential equation:

$$\rho y_{tt} + EI y_{xxxx} = \frac{ES y_{xx}}{2L} \int_0^L y_x^2 dx. \tag{1}$$

Here $y(x,t)$ is the transverse displacement of the beam point; x is a coordinate along its axis; ρ and E are the mass density and Young's modulus, respectively, of the beam; L is the length of the undeformed beam; S and I denote area and moment of inertia of the beam cross section. The nonlocal term in the right-hand side of Eq. (1) appears due to a stretching of the midplane caused by transverse displacement of the beam with immobile ends. If the bending term is negligible and both ends are clamped at distance L, then Eq. (1) reduces to the following strongly nonlinear wave equation:

$$\rho y_{tt} - \frac{ES}{2L} y_{xx} \int_0^L y_x^2 dx = 0. \tag{2}$$

This equation describes the transverse oscillations of an elastic string with fixed ends and without pretension. Only recently, a similar approximation has been developed for a discrete counterpart of such a string—a linear chain of particles moving in the plane, with next-neighbor interactions through linear springs, without pretension, and with fixed boundaries [3]. For the sake of completeness, we outline this derivation here. Let us consider a dissipation-less lattice of N particles of identical unit mass, moving in the plane and connected by linear springs with unit elastic constant (and unstretched at the horizontal position of equilibrium) and having fixed boundary conditions (cf. Fig. 1). Taking into account geometric nonlinearities, the equations of motion are [3]

$$\begin{aligned} \ddot{z}_n + T_n \cos\phi_n - T_{n+1}\cos\phi_{n+1} &= 0,\\ \ddot{y}_n + T_n \sin\phi_n - T_{n+1}\sin\phi_{n+1} &= 0,\\ n = 1,\ldots,N,\ z_1 = z_N &\equiv 0,\\ y_1 = y_N &\equiv 0, \end{aligned} \tag{3}$$

where y_n and z_n are the transverse and axial displacements of the nth particle from its equilibrium positions respectively, $v_n = n - 1 + z_n$ is the axial coordinate of the nth particle, $T_n = (r_n - l_n)$ is a stretching force (tension) in the nth spring, and l_n and r_n denote unstretched and stretched lengths of the spring respectively. In addition, ϕ_n is the angle between the nth spring and the horizontal direction, and gravity forces are neglected.

Expressing the angles and the stretching of the springs in terms of the axial and transverse deformations, and expanding in Taylor series with respect to the small differences $(z_n - z_{n-1})$ and $(y_n - y_{n-1})$ in the limit of small-energy oscillations, Eqs. (3) are reduced to the following form [3]:

$$\begin{aligned} &\ddot{z}_n - (z_{n+1} + z_{n-1} - 2z_n) - \tfrac{1}{2}(y_{n+1} - y_n)^2 + \tfrac{1}{2}(y_n - y_{n-1})^2 \\ &\quad = 0,\\ &\ddot{y}_n - (z_{n+1} - z_n)(y_{n+1} - y_n) - \tfrac{1}{2}(y_{n+1} - y_n)^3 \\ &\quad + (z_n - z_{n-1})(y_n - y_{n-1}) + \tfrac{1}{2}(y_n - y_{n-1})^3 = 0. \end{aligned} \tag{4}$$

We consider slow time scale $t \sim O(1/\varepsilon)$. Small parameter ε expresses the assumption that the energy of the system is relatively low, and the axial displacements are much smaller than the transversal ones [namely $y_n \sim O(\varepsilon)$, $z_n \sim O(\varepsilon^2)$]. At leading order of approximation the time derivative in the first equation of system (4) can be neglected, and the tension in the springs turns out to be spatially uniform and equal to

$$T_n = (z_{n+1} - z_n) + \tfrac{1}{2}(y_{n+1} - y_n)^2 = \text{const}. \tag{5}$$

*ovgend@tx.technion.ac.il

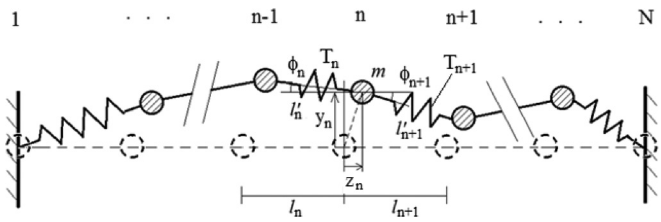

FIG. 1. The nonlinear spring-mass lattice in the plane.

Simple algebraic manipulation yields the following equation for axial tension T in the deformed chain:

$$T = \frac{1}{(N-1)}\sum_{j=0}^{N} T_j = \frac{1}{2(N-1)}\sum_{j=0}^{N}(y_{j+1}-y_j)^2. \quad (6)$$

In the last transformation fixed-fixed boundary conditions were taken into account. Note that for validity of Eq. (6) it is sufficient that only the axial displacements vanish at the chain boundaries. With account of (5) and (6), the second equation of system (4) can be rewrittten as follows:

$$\ddot{y}_n - \frac{y_{n+1}-2y_n+y_{n-1}}{2(N-1)}\sum_{j=1}^{N-1}(y_{j+1}-y_j)^2 = 0. \quad (7)$$

It is easy to recognize that Eq. (2) approximates Eq. (7) in the long-wave limit. It should be stressed here that Eq. (7) is valid only if the dynamic processes (in particular, wave propagation) are slow compared to the velocity of longitudinal sound in the chain. Besides, asymptotic regime described by Eq. (7) is settled after initial time instance, necessary for the longitudinal sound waves to pass through the chain. More details on the derivation and validity of Eq. (7) are presented in Ref. [3].

Systems (2) and (7) exemplify the important concept of *sonic vacuum*—linearization of both these systems yields zero sound velocity. Thus, these systems can be classified as *nonlinearizable*—one never can neglect the nonlinear terms. Similar properties of the sonic vacuum are well known and widely studied in systems of granular particles without external precompression; the nonlinearity appears there due to Hertzian contact [4–7]. Also, nonlinearizable systems of a different structure were widely explored as possible nonlinear energy sinks [8–11]. The essential nonlinearity of these sinks allows them to resonate with primary oscillatory systems over a broad frequency range [9] and efficiently absorb energy. Such systems are investigated as possible engineering solutions for vibration mitigation and energy harvesting in a wide range of possible applications [9,12,13].

However, systems (2) and (7), as compared to the granular media without precompression or the nonlinear energy sinks, possess an additional important property—the nonlocality. If one is interested only in modal oscillations of these systems, then the problem becomes relatively easy, since the integral term in Eq. (2) and the corresponding sum term in Eq. (7) depend only on time. Therefore, the spatial modal shapes of the strongly nonlinear sonic vacua (2) and (7) will be the same as for simple linear string or chain with fixed ends and, respectively, will correspond to sinusoidal standing waves. The nonlinearity will reveal itself only in the time domain—the oscillations will be anharmonic, and their frequency will be proportional to the amplitude [3]. The fact that the integral term in Eqs. (1) and (2) does not modify the spatial modal shapes is well known and widely used in approximate modal analysis of oscillating continuous systems [14].

II. PROPAGATION OF ACCELERATING OSCILLATORY FRONTS: SIMULATION AND THEORY

Beyond modal oscillations, the dynamics of sonic vacua similar to (2) and (7) is almost unexplored due to the strong nonlinearity. Below we demonstrate that the nonlocal nonlinearity brings about some unexpected and unusual dynamic phenomena even in very simple settings. To illustrate this, the dynamics of a spring-and-mass chain with N particles in a plane is simulated. The nondimensional Hamiltonian of the lattice is expressed as

$$H = \sum_{n=2}^{N-1}\frac{1}{2}\left(\dot{v}_n^2+\dot{y}_n^2\right) + \sum_{n=1}^{N-1}\frac{1}{2}(r_n-1)^2, \quad (8)$$

where v_n denotes the axial coordinate of the nth particle and $r_n = [(v_{n+1}-v_n)^2+(y_{n+1}-y_n)^2]^{1/2}$ is the distance between particles n and $n+1$. The right end of the chain is fixed, whereas the left end of the chain does not move in the axial (x) direction and harmonically oscillates in transversal direction. The equations of motion are expressed as

$$\begin{aligned} &v_1(t) \equiv 0, \quad y_1(t) = A\sin(\omega t),\\ &\ddot{v}_n = -\partial H/\partial v_n, \quad \ddot{y}_n = -\partial H/\partial y_n,\\ &n = 2,\ldots,N-1,\\ &v_N(t) \equiv N-1, \quad y_N(t) \equiv 0, \end{aligned} \quad (9)$$

and are numerically integrated with zero initial velocities and in straight initial configuration, by the velocity Verlet method [15] with the following parameters: $N \in [125,10000]$, excitation amplitudes $A \in [0.1,7]$, and frequencies $\omega \in [0.01,0.5]$.

Typical results of the simulation are presented in Fig. 2, where we depict the "transverse component" of local kinetic energy $E_k = \dot{y}_n^2/2$ versus n at different time instances. One can observe the propagation of the excitation front, accompanied by an apparently monochromatic oscillatory tail. Propagating fronts with oscillatory tails are well known in models of phase transitions in solid-state and similar problems [16–19]. Solitary waves on an oscillatory background (nanopterons) also involve oscillatory tails, although they propagate without energy release [20]. However, the solution presented here has a very interesting feature not known in the settings mentioned above. It follows from Fig. 2(a) that this front accelerates in the course of propagation.

To get better insight into these findings, we explore the relationship between transversal and axial oscillations for the cases examined in Fig. 2 (see Fig. 3). It is possible to see that in case (a), which corresponds to the front propagation, the kinetic energy of the axial oscillations of the lattice is about two orders of magnitude less than that of the transversal oscillations (so its omission from the plot in Fig. 2 is justified). However, in case (b), no such separation of the energy scales is observed. This latter case corresponds to the spatial localization of the boundary excitation; no accelerating oscillatory front is formed.

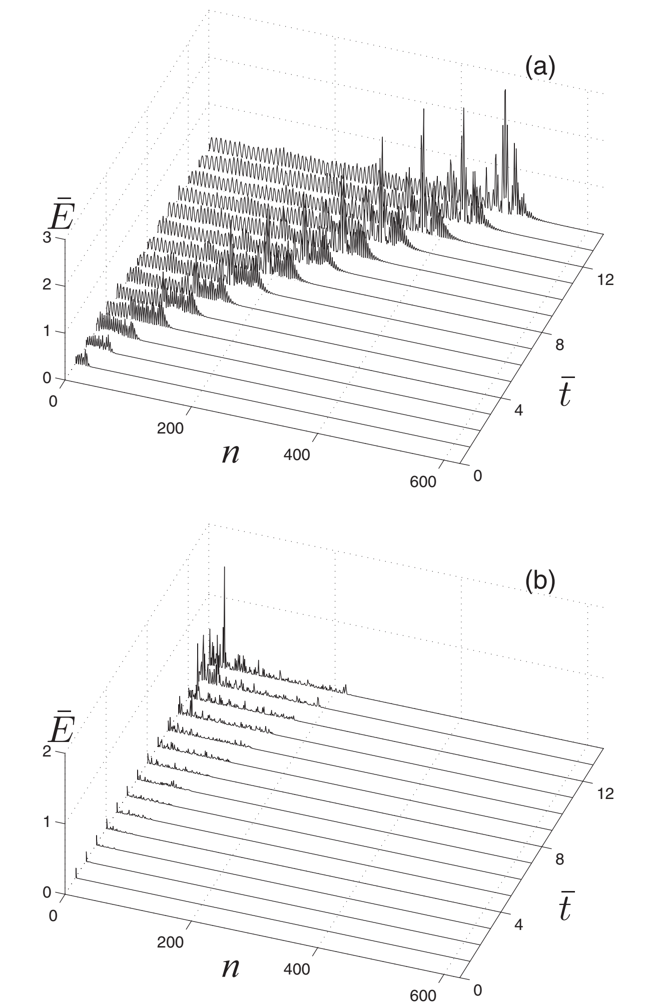

FIG. 2. Evolution of local kinetic energy $\bar{E} = \dot{y}_n^2/2\Delta E$ at different segments of time $\bar{t} = t/\Delta t$ in the chain with $N = 625$ and (a) $A = 0.5$, $\omega = 0.05$ ($\Delta E = 10^{-3}$, $\Delta t = 492$); (b) $A = 1$, $\omega = 0.3$ ($\Delta E = 1$, $\Delta t = 164$). ΔE is a rescaling coefficient for energy, introduced for better appearance of the graphs.

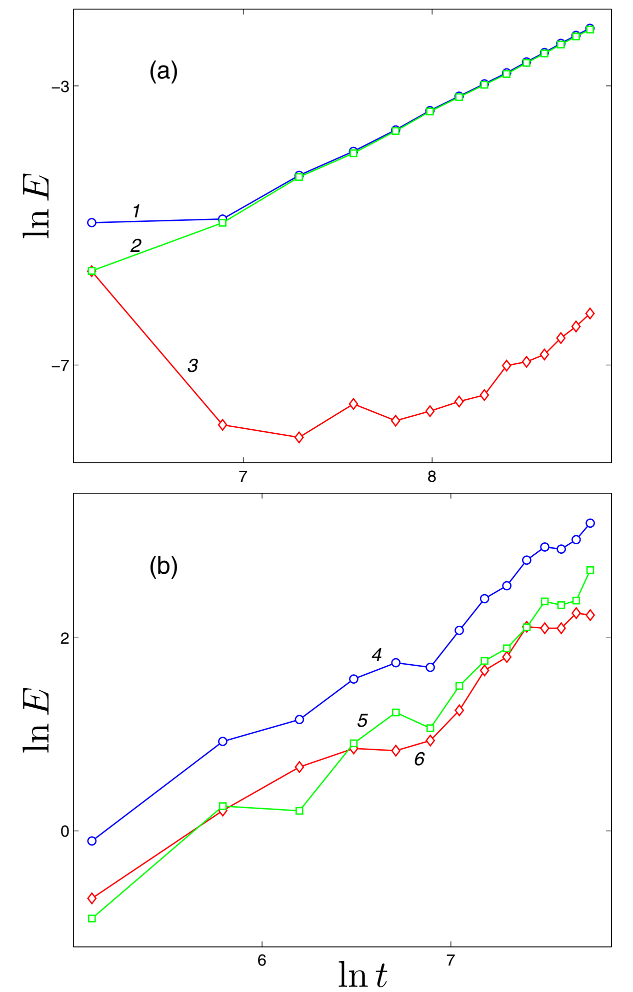

FIG. 3. Total kinetic energy (curves 1 and 4, in blue), kinetic energy of the transversal oscillations (curves 2 and 5, in green) and kinetic energy of the axial oscillations (curves 3 and 6, in red) for the chain with $N = 625$. The parameters correspond to those used for simulations presented in Fig. 2. (a) $A = 0.5, \omega = 0.05$ (front propagation); (b) $A = 1.0, \omega = 0.3$ (spatial localization close to the boundary). Both energy and time are presented in logarithmic scales.

In order to explain the observed propagation of the oscillatory front analytically, we consider a simplified model of the oscillatory region in the chain and suppose a monochromatic wave in the oscillatory tail after the front in continuum approximation. Then the field of displacements in the oscillatory zone is approximately described as follows:

$$y(x,t) = \begin{cases} A\sin(\omega t - kx), & 0 \leqslant x \leqslant l(t), \\ 0, & l(t) < x \leqslant L. \end{cases} \tag{10}$$

Here $l(t)$ is the instantaneous coordinate of the front and k is the wave number. It is also assumed at this stage that the front propagation is slow enough compared to the frequency of transverse oscillations of the particles; i.e., $dl(t)/dt \ll \omega l(t)$. To establish complete correspondence between the continuum approximation (2) and the discrete model (7)–(9), one should set $\rho = E = S = 1$, $L = N - 1$. Then, by substituting (10) to (2) and balancing principal terms, the following equation is obtained:

$$A\omega^2 \sin(\omega t - kx) \approx \frac{k^4 A^3 l(t)\sin(\omega t - kx)}{4(N-1)}. \tag{11}$$

An additional condition can be obtained from the assumed stationary character of the front propagation. To this end, the phase velocity of the oscillatory tail should be equal to the front velocity [18] so $V_{\text{ph}} = \omega/k = dl(t)/dt$. Combining this expression with Eq.(11), one obtains an explicit expression for the position of the accelerating front:

$$k^4 l(t) = \frac{4\omega^2(N-1)}{A^2} \Rightarrow \frac{1}{l}\left(\frac{dl}{dt}\right)^4 = \frac{A^2\omega^2}{4(N-1)}$$

$$\Rightarrow l(t) = Kt^{4/3}, \quad K = \left(\frac{81A^2\omega^2}{1024(N-1)}\right)^{1/3}. \tag{12}$$

Thus, the front indeed accelerates with velocity $V \sim t^{1/3}$. Wavelength of the oscillatory tail obeys the same scaling

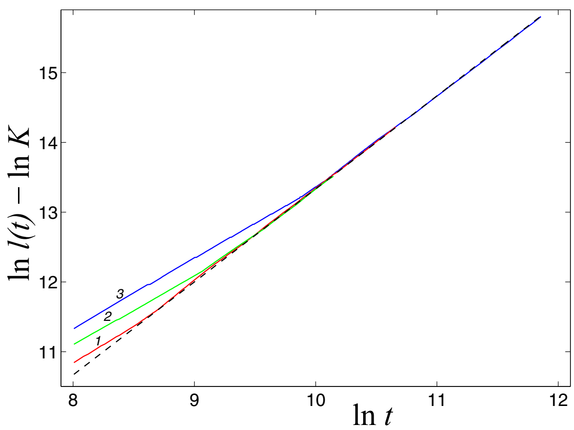

FIG. 4. Dependence of the position of the leading edge of the front $l(t)$ on time t for three different sets of parameters: $N = 2500$, $A = 0.5$, $\omega = 0.03$; $N = 5000$, $A = 1.5$, $\omega = 0.08$ and $N = 1000$, $A = 0.6$, $\omega = 0.03$ (curves 1, 2, and 3 respectively). Dashed line corresponds to the slope $t^{4/3}$.

law. Prediction of Eq. (12) is completely supported by the numerical simulations, as is demonstrated in Fig. 4, for three different sets of parameters, with the curves depicting the front position versus time (shifted by $\ln K$) collapsed into a straight line with slope 4/3. So the considerations presented above predict not only the correct scaling law for the front position but also the scaling coefficient, which depends on a specific set of parameters. One can note that coefficient K in (12) explicitly depends on the *total* chain length N, although the oscillatory front has not achieved yet the right boundary. Therefore, the nonlocality of the model is crucial for the observed acceleration of the oscillatory front.

III. INITIATION THRESHOLD FOR THE ACCELERATING OSCILLATORY FRONT

Numeric simulations presented in the previous section demonstrate that for low excitation amplitude the accelerating oscillatory front is not formed, and the zone of oscillations remains localized. From the other side, derivation presented above (10)–(12) does not imply any threshold for the front initiation and propagation. It means that the observed threshold cannot be explained in terms of the continuum model (2). Therefore, to understand these observations, one should resort to the discrete model of the chain. We will adopt a simplified approach and establish the minimal amplitude of oscillations of particle $n = 1$ that allows efficient energy transport to particle $n = 2$ and, thus, substantial excitation of the chain and initiation of the wave front. Accordingly, we analyze (7) with $y_1 = -A\sin\omega t$, $y_n = 0$, $n \geqslant 3$, and zero initial conditions for $y_2(t)$. This system is rescaled with $\omega t = \tau$, $y_2 = \alpha u(\tau)$, $A = \alpha a$, $\alpha = \omega\sqrt{2(N-1)}$. Then one arrives at the following equation for variable $u(\tau)$:

$$u_{\tau\tau} + (2u + a\sin\tau)[u^2 + (u + a\sin\tau)^2] = 0. \qquad (13)$$

One thus expects that the dynamics of the front initiation is governed by a single nondimensional parameter $a = A[\omega\sqrt{2(N-1)}]^{-1}$. The primary frequency of the oscillatory front is expected to be close to the normalized value of unity. Therefore, the complex variable $\varphi(\tau)\exp(i\tau) = u_\tau(\tau) + iu(\tau)$ is introduced [21]. Supposing that variable $\varphi(\tau)$ varies slowly, balancing principal terms in Eq. (13), we arrive at the following slow-flow equation:

$$\varphi_\tau + \tfrac{1}{2}i\varphi - \tfrac{1}{8}i[2(2\varphi + a)(|\varphi|^2 + |\varphi + a|^2) + (2\varphi^* + a)(\varphi^2 + (\varphi + a)^2)] = 0. \qquad (14)$$

Though far from obvious, this slow-flow equation is completely integrable. The integral of motion is expressed as:

$$C = |\varphi|^2 - \tfrac{1}{8}[2(|\varphi|^2 + |\varphi + a|^2)^2 + |\varphi^2 + (\varphi + a)^2|^2]. \qquad (15)$$

To see this, it is sufficient to note that Eq. (14) is equivalent to $\varphi_\tau = -\frac{i}{2}\frac{\partial C}{\partial \varphi^*}$. Since C is real, one immediately obtains $\varphi_\tau^* = \frac{i}{2}\frac{\partial C}{\partial \varphi}$ and, consequently, $\frac{dC}{d\tau} = \frac{\partial C}{\partial \varphi}\varphi_\tau + \frac{\partial C}{\partial \varphi^*}\varphi_\tau^* = 0$. Then we split the slow variable into polar components $\varphi = R\exp(i\delta)$. The initial condition $\varphi(0) = 0$ corresponds to $C = -3a^4/8$. Therefore, the averaged phase trajectories of the particle $n = 2$ for different values of the external excitation are expressed by the following family of implicit equations:

$$R^2\left(1 - \frac{3}{2}R^2 - a^2\right) - 3Ra\left(R^2 + \frac{1}{2}a^2\right)\cos\delta - 2(Ra\cos\delta)^2 = 0. \qquad (16)$$

The family of solutions of Eq. (16) for various values of a is presented in Fig. 5. One can see that for small values of a the phase trajectory stays in the region of small values of R. This regime corresponds to localization of forced oscillations near the excited end of the chain, similarly to the regime demonstrated in Fig. 2(b). There exists an excitation threshold above which the phase trajectory is attracted to a region of relatively large R. So the energy of oscillations is intensively irradiated into the chain, and it seems natural to associate this regime with the formation of the oscillatory front. The threshold excitation corresponds to the phase trajectory, which passes through the saddle point in Fig. 5 (curve 3). This yields the following evaluation for this threshold: $a_{\rm cr} \approx 0.3574$.

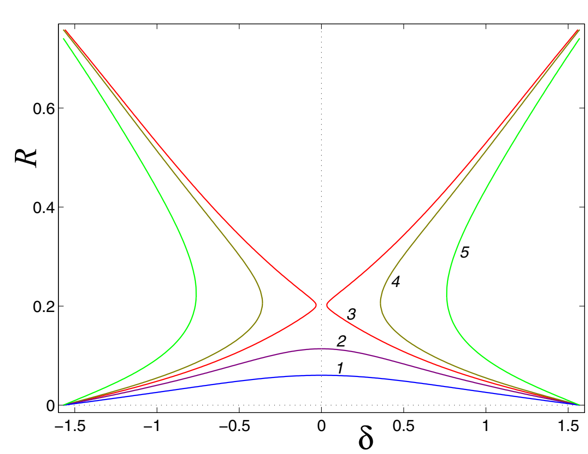

FIG. 5. Phase trajectories corresponding to Eq. (16) for zero initial conditions and $a = 0.3, 0.34, 0.3575, 0.37, 0.42$ (curves 1, 2, 3, 4, and 5 respectively).

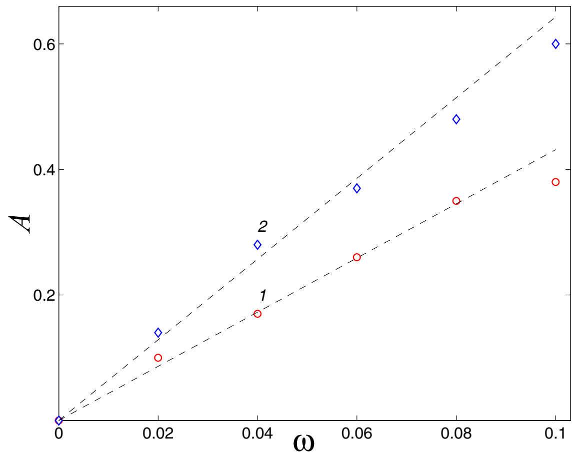

FIG. 6. Relationship between the frequency ω and the amplitude A for the oscillatory front initiation for chain lengths $N = 125$ and $N = 250$ (lines 1 and 2). The black dashed lines represent linear fitting of the markers 1 and 2. The region above a corresponding dashed line corresponds to a propagating front regime, and no front is initiated for parameters below the dashed line. The linear fitting relations are given by $A = 0.274\omega\sqrt{2(N-1)}$ for $N = 125$ and $A = 0.287\omega\sqrt{2(N-1)}$ for $N = 250$.

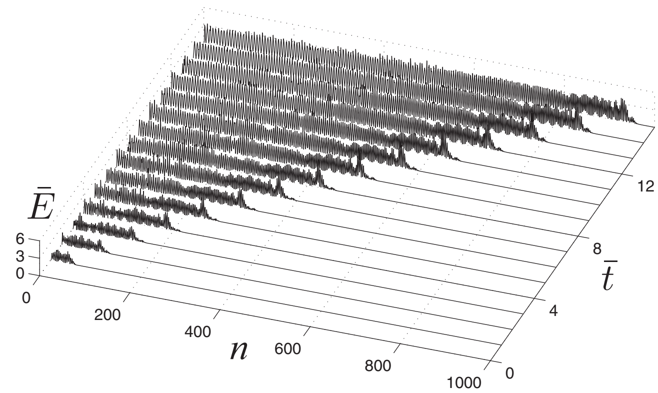

FIG. 7. Evolution of local kinetic energy $\bar{E} = \dot{y}_n^2/2\Delta E$ at different segments of time $\bar{t} = t/\Delta t$ in the chain with $N = 1500$ and $A = 0.5$, $\omega = 0.05$, $\Delta t = 792$, $\Delta E = 10^{-4}$, $\varepsilon = 0.001$.

Similar transitions are widely discussed in terms of limiting phase trajectories [21–23].

Thus, the boundary for formation of the oscillatory front is described by the line $A = a_{\mathrm{cr}}\omega\sqrt{2(N-1)}$. This prediction is verified in Fig. 6. Approximate linear dependence of A on ω is observed, but the coefficient of these lines turns out to be somewhat overestimated. This discrepancy is presumably related to the number of simplifying assumptions adopted in our analysis.

All simulations and derivations presented above explored the idealized model without bending elasticity. Experimentally, the model with negligible bending elasticity can be realized as a chain of springs linked by high-quality bearings. As one can learn from the paper, such a system can efficiently absorb energy in a wide range of frequencies when excited at sufficient amplitude. Therefore, it may be a viable candidate for the design of nonlinear energy sinks [8,9].

At the microscopic or mesoscopic level, one can consider other physical realizations of the model considered—for instance, slender microbeams or polymer macromolecules. Such systems can have some nonzero bending elasticity. Thus, it is important to establish whether the accelerating oscillatory front will exist also in this case. To check that, we simulate the chain with all conditions similar to the reported above [Eqs. (8) and (9)], but with an additional bending term in the Hamiltonian $\Delta H_b = \varepsilon\sum_{n=2}^{N-1}(1+\cos\theta_n)$, where θ_n is the angle between the neighboring links adjacent to particle n. The continuum limit of this system corresponds to Eq. (1) with $\rho = E = S = 1$, $L = N - 1$, $I = \varepsilon$. The results of this simulation are presented in Fig. 7. One can see that, at least for a relatively small bending coefficient, the accelerating oscillatory front is indeed observed. It should be mentioned that perturbation of the exact conditions of the sonic vacuum brings forward rich and interesting dynamics, which will be explored and reported elsewhere.

IV. CONCLUDING REMARKS

To conclude, we revealed a new type of excitations in a lattice representing a nonlinear sonic vacuum with strong nonlocal dynamical interactions (despite only next-neighbor physical coupling). These excitations are accelerating fronts with oscillatory tails. The fronts accelerate according to the scaling law $l \sim t^{4/3}$ due to nonlocal dynamical interactions. The tails have constant frequency, but their wavelength is not constant—it scales with time as $\lambda = 2\pi/k = 2\pi l_t/\omega \sim t^{1/3}$. Such fronts reveal themselves in most well-known and popular models, such as the suspended string without pretension and the chain of linear springs and masses with fixed ends. Simple analytic considerations allow the derivation of all main parameters of the front, including the scaling characteristics and the excitation threshold.

ACKNOWLEDGMENT

The authors are very grateful to the Israel Science Foundation (Grant No. 838/13) for financial support.

[1] L. D. Landau and E. M. Lifshitz, *Theory of Elasticity* (Pergamon Press, London, 1970).

[2] A. H. Nayfeh, *Nonlinear Interactions* (Wiley, New York, 2000).

[3] L. I. Manevitch and A. F. Vakakis, SIAM J. Appl. Math. **74**, 1742 (2014).

[4] V. F. Nesterenko, *Dynamics of Heterogeneous Materials* (Springer-Verlag, New York, 2001).

[5] C. Daraio, V. F. Nesterenko, E. B. Herbold, and S. Jin, Phys. Rev. E **73**, 026610 (2006).

[6] S. Sen, J. Hong, J. Bang, E. Avalos, and R. Doney, Phys. Rep. **462**, 21 (2008).

[7] Y. Starosvetsky, M. A. Hasan, A. F. Vakakis, and L. I. Manevitch, SIAM J. App. Math. **72**, 337 (2012).

[8] O. V. Gendelman, Nonlin. Dynam. **25**, 237 (2001).

[9] A. F. Vakakis, O. V. Gendelman, G. Kerschen, L. A. Bergman, D. M. McFarland, and Y. S. Lee, *Nonlinear Targeted Energy Transfer in Mechanical and Structural Systems* (Springer-Verlag, Berlin, 2008).

[10] L. I. Manevitch, E. Gourdon, and C. H. Lamarque, J. Appl. Mech. **74**, 1078 (2007).

[11] G. Sigalov, O. V. Gendelman, M. A. Al-Shudeifat, L. I. Manevitch, A. F. Vakakis, and L. A. Bergman, Chaos **22**, 013118 (2012).

[12] R. Bellet, B. Cochelin, P. Herzog, and P.-O. Mattei, J. Sound Vib. **329**, 2768 (2010).

[13] Z. Nili Ahmadabadi and S. E. Khadem, Mech. Mach. Theor. **50**, 134 (2012).

[14] E. Hollander and O. Gottlieb, Appl. Phys. Lett. **101**, 133507 (2012).

[15] L. Verlet, Phys. Rev. **159**, 98 (1967).

[16] D. Panja, Phys. Rep. **393**, 87 (2004).

[17] A. S. Mikhailov, *Foundations of Synergetics 1: Distributed Active Systems* (Springer-Verlag, Berlin, 1990).

[18] V. V. Smirnov, O. V. Gendelman, and L. I. Manevitch, Phys. Rev. E **89**, 050901(R) (2014).

[19] M. Schaeffer and M. Ruzzene, Int. J. Solids Struct. **56-57**, 78 (2015).

[20] M. Remoissenet, *Waves Called Solitons*, 3rd ed. (Springer Science and Business Media, Berlin, 1999)

[21] L. I. Manevitch and O. V. Gendelman, *Tractable Models of Solid Mechanics* (Springer-Verlag, Heidelberg, 2011).

[22] L. I. Manevitch, A. S. Kovaleva, E. L. Manevitch, and D. S. Shepelev, Commun. Nonlinear Sci. Numer. Simul. **16**, 1089 (2011).

[23] L. I. Manevitch, Appl. Math. Sci. **9**, 4269 (2015).